JECS 1806c
Journal of the European Ceramic Society 17 (1997) 587–592

PII: S0955-2219(96)00101-X
0955-2219/97/$17.00

The Effect of Heat-Treatment on the Performance of Sub-Micron SiC_p-Reinforced α-β Sialon Composites: II. Heat-Treatment Studies

Q. Liu,[a] L. Gao,[a] D. S. Yan,[a] H. Mandal[b] & D. P. Thompson[c]

[a]Shanghai Institute of Ceramics, Chinese Academy of Sciences, Shanghai 200050, People's Republic of China
[b]Department of Ceramic Engineering, Anadolu University, Eskisehir, Turkey
[c]Materials Division, Dept of Mechanical, Materials and Manufacturing Engineering, University of Newcastle upon Tyne, NE1 7RU, UK

(Received 3 July 1995; revised version received 21 May 1996; accepted 30 May 1996)

Abstract

The effects of heat-treatment on $\alpha \rightarrow \beta$ sialon transformation in dense, agglomerate-free Ln-sialon/SiC_p(Ln=Nd, Yb) composites are reported. The stability of the α-sialon phase is not only dependent on the temperature and time of heat-treatment, but also on the kind of additive and the amount of SiC particles. In Nd-densified samples, the α-sialon phase is very unstable at 1450°C and transforms almost totally to the β phase with the Nd-M (melilite) phase and $NdAlO_3$ as grain-boundary crystalline phases. In contrast, Yb^{3+}-densified samples show good stability for the α-sialon phase at 1450°C, with only a small amount of β-sialon produced. The crystalline grain-boundary phases produced in this case are Yb-garnet, and Yb-J-phase. © *1997 Elsevier Science Limited. All rights reserved.*

1 Introduction

The incorporation of sub-micron silicon carbide particles into ceramic matrices has been the subject of intense study in recent years because, during sintering of these materials, the matrix phase accommodates the SiC particles not only in grain boundaries but also within sintered grains, thus allowing more complex failure mechanisms to operate, with significant benefits to mechanical properties, especially bend strength. The present series of papers takes on board the overall principles of previous work on Si_3N_4–SiC composites,[1–6] and applies them very specifically to the case of SiC_p-containing α-β sialon ceramics, because it has recently been demonstrated that the microstructure of these materials can be substantially changed by $\alpha \rightarrow \beta$ sialon transformation at temperatures in the range 1300–1600°C.[7] Not only does the transformation afford the possibility of changing from a microstructure consisting of hard equiaxed α-sialon grains, to the stronger, tougher needle-shaped microstructure of β-sialon, but also the grain refinement as α grains fragment into a very fine-grained mixture of β-sialon plus other glassy or crystalline phases allows higher-strength composites to be produced. Recent studies have shown that $\alpha \rightarrow \beta$ sialon transformation proceeds at different rates when different Ln_2O_3 densification additives are used, leading to the formation of different microstructures. There is therefore an enormous range of parameters which can be adjusted for property optimisation. The simultaneous presence of nano-size silicon carbide grains in the microstructure allows further possibilities for microstructural modification,[8,9] with possibly different behaviour resulting depending whether the SiC grains are incorporated into the α- or the β-sialon grains because of their different morphologies.

The first paper in the present series[10] demonstrated how a uniform, non-agglomerated dispersion of sub-micron silicon carbide particles could be introduced into mixed α-β sialon ceramics by controlled chemical procedures, using PEG (polyethylene glycol) as a surfactant. Hot-pressing of these materials resulted in the formation of fully dense products containing isolated sub-micron grains of silicon carbide, generally located at the grain boundaries between α and β grains. This, the second paper in the series, describes the heat-treatment of materials prepared in the first study, with the aim of facilitating $\alpha \rightarrow \beta$ sialon transformation, and exploring changes in the resulting microstructure. This has been explored for the two cases of Nd and Yb as the densifying additives, for compositions containing either 0, 10 or 20 wt% of sub-micron SiC particles.

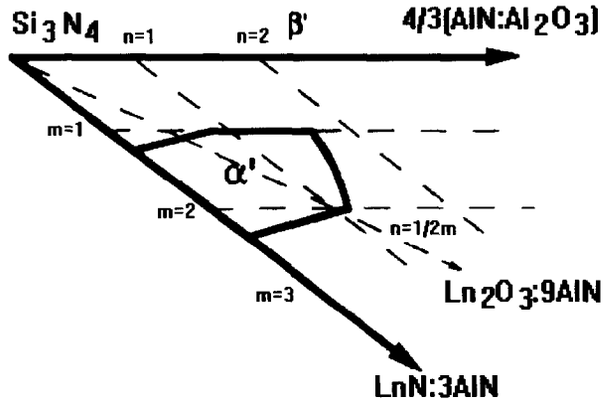

Fig. 1. Schematic representation of the α-sialon plane in Ln–Si–Al–O–N systems.

2 Experimental Procedure

Starting compositions were selected corresponding to values of $m = 1{\cdot}0$ and $n = 1{\cdot}7$ in the general α-sialon formula $Ln_xSi_{12-m-n}Al_{m+n}O_nN_{16-n}$ where $x = 0{\cdot}3333$ (Fig. 1). Ln was chosen to be Nd and Yb, because previous work has established that the α-sialon structure is stable for elements with atomic numbers larger than cerium (Z = 58) and these are essentially the two end members.[7,11–13] Sub-micron SiC powders (Ibiden Co., Japan) of mean particle size 280 nm were incorporated into the sialon mixes to the extent of either 0, 10 or 20 wt%. Details of the preparation procedure, including the use of PEG to avoid agglomeration of the SiC powder have been described in the previous paper.[10]

Cylindrical green pellets of the mixed powders were compacted by applying uniaxial pressure in steel dies 25 mm in diameter and the resulting pellets were isostatically pressed. The discs were hot-pressed at 1800°C for 45 min under a pressure of 30 MPa. As-sintered samples were heat-treated in an alumina tube furnace in flowing nitrogen at 1450°C for one day and four days respectively to modify the microstructure and change the α/β sialon ratio. Densities were measured with a mercury displacement balance, using Archimedes' principle. Phase identification was carried out by X-ray diffraction using a Hagg-Guinier focusing camera with Cu K_{α_1} radiation, using the intensities of the (102) and (210) peaks of the α-sialon phase and the (101) and (210) peaks of the β-sialon phase for quantitative estimation of phase content. TEM and SEM microstructural studies were carried out using JEOL-TEM (JEOL-200CX) and Cam-Scan SEM (S4-80DV) instruments, the latter equipped with EDX facilities and a windowless detector suitable for light-element analysis. The specimens for SEM observation were ground, polished, and gold-coated. The SEM micrographs were then used for measurement of grain size, grain shape, and phase distribution. The specimens for TEM were prepared as follows. The sintered discs were cut with a diamond saw into slices. These slices were polished down to a thickness of 300 μm and given a concave lapping to a thickness of about 10 μm in the thinnest region. Then, the specimens were thinned by argon ion sputtering until perforation occurred. Details of location of SiC particles, grain boundary phases, $\alpha \rightarrow \beta$ transformation, etc. were characterised by High Resolution Transmission Electron Microscopy (HRTEM).

3 Results and Discussion

3.1 Characterisation of the sintered composites

Dense, agglomerate-free $SiC_{(p)}$/Ln–sialon(Ln = Nd and Yb) composites were obtained by hot-pressing at 1800°C. Examination of polished cross-sections by SEM showed that only a few micropores were present, indicating that the samples had reached essentially theoretical density. As regards the effectiveness of the dispersion of SiC_p in the material, these micrographs showed that the chemical methods reported in the previous paper[10] had been successful in preventing agglomeration of the sub-micron SiC particles.

The results show that Yb_2O_3 gives higher densities in SiC_p/Ln-sialon composites than Nd_2O_3. Table 1 lists selected characteristics of these materials. In the Nd-densified sample, there is slightly more β-sialon than α-sialon, and the aluminium-containing melilite(M') phase appears as a crystalline phase at the grain boundaries plus also some glassy phase. The distribution of phases is clearly identified from the contrast on the micrographs shown in Fig. 2, where β-sialon grains are black, α-sialon grains are grey and grain-boundary phases are white. It has been found that M' phase is usually an intermediate product in the sintering of Nd–α-sialon material and incorporates high levels of neodymium into its structure. Therefore, not only is it difficult to achieve high proportions of α-sialon in the final product, but also the densification of the composites is considerably retarded because of the high melting point of the Nd-M'

Table 1 Densities and β/α sialon ratios for as-sintered Ln-sialon/SiC_p composites.

	0 wt% SiC_p		*10 wt% SiC_p*		*20 wt% SiC_p*	
	Nd-system	*Yb-system*	*Nd-system*	*Yb-system*	*Nd-system*	*Yb-system*
d(g/cm^3)	3·35	3·42	3·33	3·39	3·30	3·37
β/α ratio	55/45	6/94	52/48	10/90	53/47	6/94

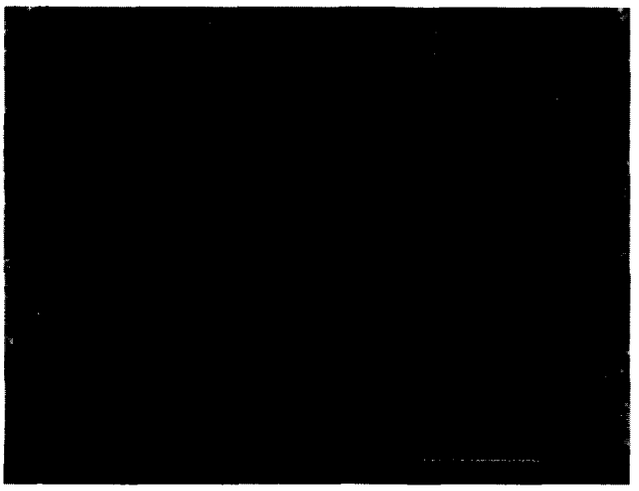

(a)

(b)

Fig. 2. SEM micrographs of sintered Ln-sialon/SiC_p composites: (a) Nd-system and (b) Yb-system.

phase.[14–17] Comparatively, the Yb-doped composite produced under the same conditions as the Nd sample, was more dense, and contained only some glassy phase at the grain boundaries. Clearly, the smaller Yb^{3+} cations (r_{Yb3+} = 0·886Å) form a more stable α-sialon phase than Nd^{3+} (r_{Nd3+} = 0·995Å) at lower temperatures (1200–1500°C) so that some transformation of the latter to β-sialon occurs on cooling. The radius of the rare earth cation is only one of the factors influencing the stability of the α-sialon structure; other factors include the solubility of cations in the structure, the viscosity and wettability of grain boundary liquid phase, heat-treatment conditions, etc.

3.2 Effects of heat-treatment on the transformation

All samples sintered at 1800°C were heat-treated at 1450°C in flowing nitrogen for 24 and 96 h, respectively. The resulting phases are listed in Table 2. After the long heat-treatment at 1450°C, much more α-sialon transformed to β-sialon in Nd-densified

Table 2 Characteristics of Ln-sialon/SiC_p composites after heat treatment

	0 wt% $SiC_{(p)}$		*10 wt% $SiC_{(p)}$*		*20 wt% $SiC_{(p)}$*	
	Nd-system	*Yb-system*	*Nd-system*	*Yb-system*	*Nd-system*	*Yb-system*
d(g/cm^3)	3·33*	3·41*	3·29*	3·38*	3·30*	3·33*
	3·27**	3·39**	3·31**	3·39**	3·28**	3·29**
β/α	66/34*	12/88*	74/26*	19/81*	82/18*	15/85*
	100/00**	10/90**	100/0**	20/80**	91/9**	12/88**
Crystal phases	M'	G	M'	G	M'	G
	A	Y	A	Y	A	Y

M' = Aluminium-containing melilite ($Nd_2Si_3Oa_4N_3$);
A = Neodymium aluminate ($NdAlO_3$)
G = Ytterbium aluminium garnet ($Yb_3Al_5O_{12}$)
Y = Ytterbium J-phase ($Yb_4Si_2O_7N_2$)
* = Heat treatment, 1450°C, 24 h;
** = Heat treatment, 1450°C 96 h.

samples than in the equivalent Yb-densified samples. These experiments show that the $\alpha \rightarrow \beta$ transformation in Ln-sialon/SiC_p samples is dependent on temperature, time, the type of additive and also on the amount of SiC_p added. Thus for Nd-densified samples, the as-sintered materials show similar β:α ratios regardless of SiC content, whereas after 24 h of heat-treatment, the β content steadily increases. After 96 h of heat-treatment, samples are completely converted to β with the exception of the 20% SiC_p sample, which still retains a small amount of α-sialon. Whereas the increase in β content in the 10% SiC samples can be attributed to the additional silica (on the surface of the SiC_p grains) which increases the amount and reduces the viscosity of liquid phase, the retained α in the 20% SiC sample can be explained more in terms of the large numbers of SiC particles interrupting diffusion paths through the microstructure.

The Yb-densified samples are influenced by the larger amount of β in the as-sintered 10% SiC samples. Apart from this, the β:α ratio doubles in each sample after 24 h of heat-treatment, and thereafter remains constant. This doubling can be attributed to the change in liquid composition and modified phase relationships at the lower temperature compared with at the hot-pressing temperature. The Yb α-sialon composition is clearly stable in equilibrium with the liquid phase and no further change occurs as a function of time. The higher β content in the as-sintered 10% SiC sample may be due to slight changes in processing conditions for this sample.

After heat-treatment for 96 h, grain boundary phases have thoroughly crystallized in the two systems. For Nd-doped composites, Nd-M' and $NdAlO_3$ phases are dominant, whereas Yb-garnet

and Yb-J phase exist in the Yb-system as grain-boundary phases, the amount depending on the viscosity and crystallization rate of these phases under the heat-treatment conditions. The results agree with reports by other authors[18] and also with our own TEM and EDAX analysis.

The effect of SiC_p additions on $\alpha \rightarrow \beta$ sialon transformation in heat-treated materials is not strongly marked. In the case of Nd-densified materials, there is a slight increase with increasing SiC content, but for Yb-densified materials there is very little change. The 20% SiC_p-containing Nd-sample showed some evidence that the SiC particles hinder the diffusion of material associated with the transformation, but further work is necessary to come to a quantitative conclusion on this point. It is certainly well known[19] that small additions of sub-micron SiC particles hinder the densification of oxide and nitride ceramics and extending this principle to $\alpha \rightarrow \beta$ sialon transformation is a logical step.

3.3 $\alpha \rightarrow \beta$ sialon transformation

$\alpha \rightarrow \beta$ Sialon transformation has been an important new research topic in sialon ceramics and mechanisms for this are currently being investigated. The transformation is regarded as a process of solution-diffusion-precipitation, i.e. solution of α-sialon, diffusion of atoms through a grain-boundary oxynitride liquid, followed by precipitation of β-sialon from the liquid.[20–23] The experimental evidence for solution-diffusion-precipitation has been gathered from two sources. One is the distribution profile of the solute concentration across β-sialon grains. The relative Al concentration is higher in the centre than at the edges of the grains, and higher in areas adjacent to the liquid pocket than at the narrow grain boundaries; this means that the anisotropic growth of β grains is due to the difference in local solute diffusivity.[24,25] Another discussion point is whether β grains precipitate on existing α- or β-sialon cores or in some other location. Some reports have concluded that pre-existing α cores provide nucleation sites for β growth[26–28] but the idea of self-nucleation of the $\alpha \rightarrow \beta$ transformation has been proposed by other authors.[21–23,29] Recently, Hirai *et al.*[30] studied shock-compacted Si_3N_4 nanocrystalline ceramics. They found that surface melting of the individual grains propagated into the centre as temperature increased, and a large mass formed. Finally a precursor of β emerged from the mass and grew into a large β-sialon crystal.

In the present study, pure α-sialon was selected as the matrix for obtaining microstructural evidence for $\alpha \rightarrow \beta$ sialon transformation in agglomerate-free SiC_p-reinforced sialon composites. TEM was used to achieve the higher resolution needed to infer information about the $\alpha \rightarrow \beta$ transformation mechanism. It has been considered that the nucleation sites for β, in the form of either cores or inside the liquid region depend on the circumstances in which the transformation is induced. If β grains homogeneously precipitate from lower-viscosity glassy phases at the pockets of grain junctions, they have no cores and always develop

Fig. 3. TEM image of elongated β-sialon grains without cores.

Fig. 4. TEM image of an equiaxed β-sialon grain with small cores.

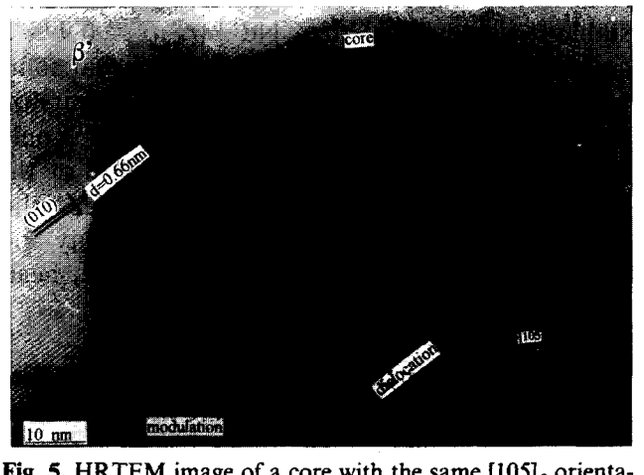

Fig. 5. HRTEM image of a core with the same $[105]_\beta$ orientation as the β-sialon grain surrounding it. There are a few lattice defects (dislocations and moiré patterns - as indicated by arrows) at the edge.

an elongated morphology; alternatively they may precipitate on impurities or SiC particles, and in this case display a different grain morphology. Figure 3 is a TEM micrograph showing no cores inside the elongated β-sialon grains. If a few α grains, all in similar orientations, partially dissolve during heat treatment leaving only small α cores, β-sialon will heterogeneously precipitate on the surfaces of the cores and grow into large crystals, with the same crystal faces dominant as in the original α-sialon cores. Figure 4 shows a β-sialon grain grown from cores with an apparently equiaxed morphology. Furthermore, HRTEM techniques give direct lattice images which further support these conclusions. Figure 5 shows a TEM micrograph, from which the d-spacings of the lattice planes can be assigned to the (010) planes of β; the corresponding diffraction pattern is attached. The outline of the core is smooth and featureless with few defects (dislocations and moiré patterns) around it (indicated by arrows). Although it was impossible to identify the composition and phase of the core by selected area diffraction or EDX, it is clear that the core has a similar crystal lattice to the surrounding β-sialon grain, causing the β grain to grow in a [105] orientation. β-sialon grains can also precipitate on impurities and SiC particles.

4 Conclusions

(1) The stability of α-sialon in agglomerate-free SiC_p-reinforced sialon composites is not only sensitive to the temperature and time of heat-treatment, but also to the kind of additives and to the amount of SiC particles present.

(2) After longer heat-treatment times, Nd α-sialon of composition $m = 1$, $n = 1{\cdot}7$ is unstable and almost totally transforms to β-sialon with Nd-M' (melilite) and $NdAlO_3$ as grain boundary crystalline phases. In contrast the smaller Yb^{3+} cation is a much more effective additive for α-sialon stability, i.e. α-sialon remains substantially untransformed in the Yb-sample, with only trace amounts of β-sialon plus Yb-garnet, and Yb-J-phase in the grain boundaries.

(3) It was found that in Nd-densified samples the β/α ratio uniformly increased with increasing additions of SiC_p up to 20 wt% reaching 100:0 in 0 and 10% SiC_p samples 91:9 in the 20% SiC_p sample. Since $\alpha \rightarrow \beta$ transformation is via a solution-diffusion-precipitation process, SiC particles located at grain boundaries may hinder diffusional flow of material when present in large amounts, but may assist the transformation when present in small amounts because their surface silica content increases the volume of liquid phase. In Yb-densified samples, the SiC_p grains had very little effect because of the increased stability of the α-sialon phase in this system.

(4) Nucleation sites for β-sialon depend on the local circumstances under which $\alpha \rightarrow \beta$ transformation is taking place. When the β phase precipitates from low-viscosity glassy phases at the pockets of grain junctions, β grains always homogeneously precipitate with an elongated morphology and without a central core. When β precipitates from fully or nearly completely dissolved α grains, it usually adopts an equiaxed morphology with α or β cores in the centre of the grains.

Acknowledgements

This work was supported by the Royal Society in the United Kingdom and the State Key Lab of High Performance Ceramics and Superfine Microstructure at the Shanghai Institute of Ceramics, People's Republic of China. Helpful discussions with Prof. S. L. Wen of the Shanghai Institute of Ceramics are greatly appreciated.

References

1. Akimune, Y., Ogarawara, T. & Hirosaki, N., Influence of starting powder characteristic on mechanical properties of SiC-particle/Si_3N_4 composites. *J. Ceram. Soc. Jpn*, **100** (1992) 463–467.
2. Akimune, Y., Hirosake, N., Ogasawara, T., *et al.*, Mechanical properties of SiC-particle/sialon composites. *J. Mater. Sci. Lett.*, **10** (1991) 223–226.
3. Niihara, K., New design concept of structural ceramics — ceramic nanocomposites. *J. Ceram. Soc. Jpn*, **99** (1991) 974–982.
4. Akimune, Y., High-temperature strength of SiC whisker sialon composites. *J. Mater. Sci. Lett.*, **9** (1990) 816–817.
5. Niihara, K., Nanostructure design and mechanical properties of ceramic composites. *J. Jpn Soc. Powder and Powder Metall.*, **37** (1990) 348–351.
6. Buljam, S. T., Pasto, A. E. & Kim, H. J., Ceramic whisker- and particulate-composites: properties, reliability, and applications. *Am. Ceram. Soc. Bull.*, **68** (1989) 387–394.
7. Mandal, H., Thompson, D. P. & Ekstrom, T., Reversible $\alpha = \beta$ sialon transformation in heat-treated sialon ceramics. *J. Eur. Ceram. Soc.*, **12** (1993) 421–429.
8. Greskovich, C. & Palm, J. A., Observations on the fracture toughness of β-Si_3N_4–β-SiC composites, *J. Am. Ceram. Soc.*, **63** (1980) 597–599.
9. Lange, F. F., Effect of microstructure on the strength of Si_3N_4–SiC composite system, *J. Am. Ceram. Soc.*, **56** (1973) 445–450.
10. Liu, Q., Gao, L., Yan, D. S., Mandal, H. & Thompson, D. P., The effect of heat-treatment on the performance of sub-micron SiC_p-reinforced α-β sialon composites: I. Preparation of agglomerate-free starting powders (this volume).
11. Sun, W. Y., Tien, T. Y. & Yen, T. S., Solubility limits of α'-sialon solid solutions in the system Si,Al,Y/N,O. *J. Am. Ceram. Soc.*, **74** (1991) 2547–2550.

12. Mandal, H., Thompson, D. P. & Ekstrom, T., Heat treatment of sialon ceramics densified with higher atomic number rare earth and mixed yttrium/rare earth oxides. *Proc. Special Ceramics 9*, The Institute of Ceramics, Stoke-on-Trent, UK, 1992, pp. 97–104.
13. Mandal, H., Thompson, D. P. & Ekstrom, T., Heat treatment of Ln–Si–Al–O–N glasses. *Proc. 7th Irish Mater. Forum Conf. IMF7*, ed. M. Buggy & S. Hampshire. Trans Tech. Publications, Switzerland, 1992, pp. 187–203.
14. Cheng, Y. B. & Thompson, D. P., Pressureless sintering and phase relationship of samarium α-sialon. *J. Eur. Ceram. Soc.*, **14** (1994) 343–349.
15. Cheng, Y. B. & Thompson, D. P., Aluminum-containing nitrogen melilite phases. *J. Am. Ceram. Soc.*, **77** (1994) 143–148.
16. Cheng, Y. B. & Thompson, D. P., Preparation and grain boundary devitrification of samarium α-sialon ceramics. *J. Eur. Ceram. Soc.*, **14** (1994) 13–21.
17. Mandal, H., Cheng, Y. B. & Thompson, D. P., α-Sialon ceramics with a crystalline melilite grain-boundary phase. *Proceedings of the 5th International Symposium on Ceramic Materials and Components for Engines*, ed. D. S. Yan, *et al.* World Scientific, 1994, pp. 202–205.
18. Ekstrom, T. & Shen, Z. J., Temperature stability of rare earth doped α-sialon ceramics, *Proceedings of the 5th International Symposium on Ceramic Materials and Components for Engines*, ed. D. S. Yan, *et al.* World Scientific, 1994, pp. 206–210.
19. Wada, H., Wang, M. J. & Tien, T. Y., Stability of phases in the Si–C–N–O system. *J. Am. Ceram. Soc.*, **71** (1988) 837–840.
20. Lange, F. F., Relation between strength, fracture energy and microstructure of hot-pressed Si_3N_4. *J. Am. Ceram. Soc.*, **56** (1973) 518–522.
21. Natansohn, S. & Sarin, V. K., The α-to-β transformation in Si_3N_4 powder. *Proceedings of the Second International Conference Ceramic Powder Processing Science*, ed. H. Hansner, *et al.* Deutsche Keramische Gesellschaft, Köln, Germany, 1989, pp. 433–444.
22. Hwang, C. J. & Tien, T. Y. Microstructural development in sialon nitride ceramics. *Materials Science Forum*, **47** (1989) 84–109.
23. Hampshire, S. & Jack, K. H., The kinetics of densification and phase transformation of nitrogen ceramics. *Proc. Brit. Ceram. Soc.*, **31** (1981) 37–49.
24. Bonnell, D. A., Ruhle, M. & Tien, T. Y., Redistribution of aluminum ions during processing of sialon ceramics. *J. Am. Ceram. Soc.*, **69** (1986) 623–627.
25. Kim, N. K., Kim, D. Y., Kranzmann, A., *et al.*, Variation of Al concentration in β-sialon grains formed during liquid phase sintering of Si_3N_4–Al_2O_3–Nd_2O_3. *J. Mater. Sci.*, **28** (1993) 4355–4358.
26. Chatfield, C., Ekstrom, T. & Mikus, M., Microstructural investigation of alpha-beta yttrium sialon materials. *J. Mater. Sci.*, **21** (1986) 2297–2307.
27. Ingelstrom, N. & Ekstrom, T., Relation between composition, microstructure and cutting tool performance of alpha-beta sialons. *J. Phys.*, **47** (1986) 347–352.
28. Ekstrom, T., Ingelstrom, N., Brage, R., *et al.* α-β Sialon ceramics made from different silicon nitride powders. *J. Am. Ceram. Soc.*, **71** (1988) 1164–1170.
29. Han, S. M., Kang, S. J. L. & Lee, Y. T., Phase transformation from α- to β-sialon by liquid infiltration in Y–Si–Al–O–N system. *J. Eur. Ceram. Soc.*, **12** (1993) 431–434.
30. Hirai, H. & Kondo, K. I., Shock-compacted Si_3N_4 nanocrystalline ceramics: mechanisms of consolidation and of transition from α- to β-form. *J. Am. Ceram. Soc.*, **77** (1994) 487–492.